

INFLUENCE OF LARGE DEFLECTION ON THE MEASUREMENT OF BENDING PROPERTIES OF VENEER BY THREE-POINT STATIC BENDING TESTS

Hiroshi Yoshihara

Associate Professor
Department of Natural Products Resource Engineering
Shimane University
Matsue, Shimane, Japan

and

Atsushi Itoh

Former Student
Department of Natural Products Resource Engineering
Shimane University
Matsue, Shimane, Japan

(Received March 2002)

ABSTRACT

We conducted three-point bending tests of specimens with span/depth ratios larger than those used in the major standards, and examined the influence of deflection on the measurement of bending properties. The specimens were taken from Western hemlock (*Tsuga heterophylla* Sarg.) and buna (Japanese beech, *Fagus crenata* Endl.). Bending tests were conducted with the specimens whose span/depth ratios varied from 20 to 140. Bending stress was calculated by the equation based on elementary bending theory and that in which the influence of deflection is taken into account, whereas the strain at the center of the bottom plane was obtained from the deflection and strain gage output. The bending stress-strain relations obtained from the different procedures were compared with each other, and the influence of deflection on the measurement of bending properties—Young's modulus, proportional limit stress, and bending strength—were examined. In addition to the bending tests, simple numerical analyses considering the material nonlinearity were conducted, and the results were compared with those obtained from the bending tests. We found that the deflection had a small influence on the measurement of Young's modulus and proportional limit stress. In contrast, the bending strength obtained by elementary bending theory decreased when the span/depth ratio exceeded 100, whereas that given by the equation considering the deflection was stable throughout the span/depth ratio range examined here. The stress-strain relation given by the numerical analysis showed a rather good approximation of the one obtained from the bending test.

Keywords: Bending test, deflection, span/depth ratio, elementary bending theory, numerical analysis.

INTRODUCTION

For the effective utilization of wood resources, the demand for products fabricated by bonding thin wooden materials such as plywood and laminated veneer lumber (LVL) needs to be markedly increased. To develop a design methodology for these products, it is important to know the mechanical properties of materials made of these products, for which the bending test is one of the most effective

methods. When bending a thin specimen, failure does not occur in the small deflection condition, and so elementary bending theory, which is usually used for evaluating bending properties, is not applicable because of the finite deformation and the change in the direction of reaction force at the supporting point. Although the span/depth ratio standardized in the major standards is specified not to be influenced by the deflection (ASTM D143-94, 1997; ISO 3349-75, 1975; JIS Z2101-94,

TABLE 1. Crosshead speed corresponding to each test span.

Test span (mm)	Crosshead speed (mm/min)
100	1.0
200	5.0
300	10
400	20
500	40
600	60
700	80

1994), bending properties of specimens with large span/depth ratio cannot be obtained properly without considering the influence of deflection. Nevertheless, there have been few studies on the influence of deflection on measuring the bending properties of wood.

In this research, we conducted three-point bending tests (center point load application) using specimens with span/depth ratios larger than the standardized ones, and examined the influence of deflection on the measurement of Young's modulus, proportional limit stress, and bending strength. In addition to the bending tests, the influence of deflection was examined by numerical analyses taking into account the material nonlinearity.

EXPERIMENT

Materials

Buna (a kind of Japanese beech, *Fagus crenata* Endl.) and western hemlock (*Tsuga heterophylla* Sarg.) were used for the specimens. The density of beech was 0.65 g/cm³, whereas that of hemlock was 0.45 g/cm³. Specimens were cut from the same lumber, and were conditioned at 20°C and 65% relative humidity before and during the tests. The dimensions of cross section were 20 and 5 mm in the radial and tangential directions, respectively, and the specimens were tested in the flatwise orientation, whereas the length in the longitudinal direction was 150 mm longer than the span length mentioned below. Five were used for each testing condition.

Bending tests

Three-point bending tests were undertaken by varying the span lengths, and Young's modulus, proportional limit stress, and bending strength corresponding to the span/depth ratio were obtained. Since the span length (l) varied from 100 to 700 mm at intervals of 100 mm, the span/depth ratio varied from 20 to 140, which is larger than those used in the major standards; 14 in the ASTM and JIS, and 12–16 in the ISO (ASTM D143-94, 1997; ISO 3349-75, 1975; JIS Z2101-94, 1994). The radius of the supporting point was 10 mm, whereas that of the loading nose was 15 mm. The vertical load was applied to a longitudinal-radial plane of the specimen. The constant load rates used are shown in Table 1 and were determined such that the strain rate at the center did not exceed 0.005/min so that specimen broke after approximately 5 min. The strain gage (Tokyo Sokki FLA-2-11, gage length = 2 mm) was bonded on the longitudinal-radial plane opposite to the loading points. The load P , loading period, and strain at the center ϵ_g were recorded by a data log (Tokyo Sokki TDS-303) at intervals of 5 s. The deflection δ at the midspan was calculated by multiplying the crosshead speed by the instantaneous time.

Bending stress was calculated from the equation based on elementary bending theory and that in which the deflection is taken into account. The bending stress derived from elementary bending theory is defined as σ_{eb} and is represented as follows:

$$\sigma_{eb} = \frac{3Pl}{2wh^2} \quad (1)$$

where w and h are the width and height of specimen, respectively. In contrast, there are several equations in which the deflection is taken into account (Uemura et al. 1978; Uemura 1981). In this research, we examined the equation standardized in the JIS (JIS K7074-88, 1988), which is defined as σ_{ld} and given by

$$\sigma_{ld} = \frac{3Pl}{2wh^2} \left[1 + 4 \left(\frac{\delta}{l} \right)^2 \right] \quad (2)$$

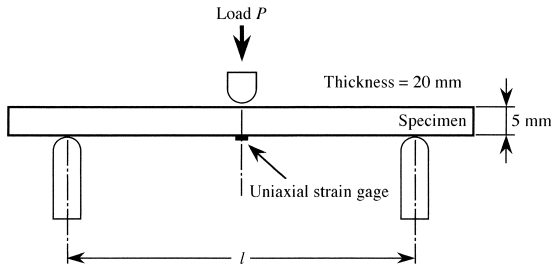


FIG. 1. Diagram of static bending tests.

When δ is obtained from the strain gage output ε_g , it is derived as follows:

$$\delta = \frac{l^2}{6h} \varepsilon_g \quad (3)$$

Strain in the longitudinal direction was directly obtained from the strain gage output ε_g and from the loading point displacement. The strain obtained from the loading point displacement is defined as ε_{dl} and is derived by elementary bending theory as follows:

$$\varepsilon_{dl} = \frac{6h}{l^2} \delta \quad (4)$$

By the stress σ_{eb} and σ_{ld} and strain ε_{dl} and ε_g , four stress-strain relations $\sigma_{eb}-\varepsilon_{dl}$, $\sigma_{eb}-\varepsilon_g$, $\sigma_{ld}-\varepsilon_{dl}$, and $\sigma_{ld}-\varepsilon_g$ were obtained.

The bending strength σ_{max} was derived from the maximum stress obtained from Eqs. (1) and (2). Young's modulus was calculated by regressing the stress-strain relation into Ramberg-Osgood's function represented as follows (Ramberg and Osgood 1943):

$$\varepsilon = \frac{\sigma}{E} + \beta \left(\frac{\sigma}{\sigma_{max}} \right)^n + c \quad (5)$$

where E is Young's modulus, β and n are the material parameters, and c is the offset strain. Figure 2 shows the diagram of stress-strain relation. The proportional limit stress σ_{pl} was determined from the intersection point of Eq. (5) and the straight line with the inclination of 3% reduced Young's modulus. The equation with the reduced modulus is represented as:

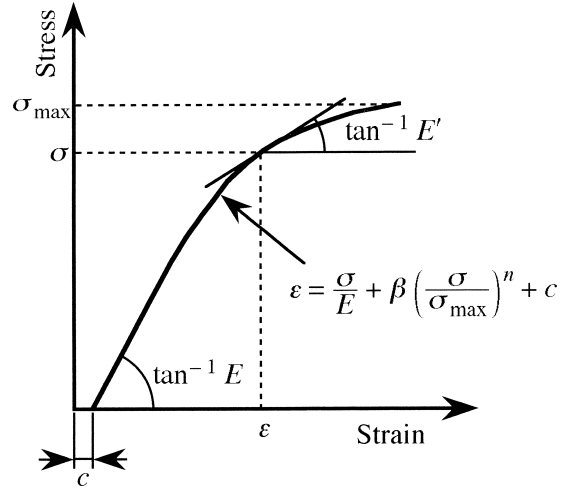


FIG. 2. Stress-strain relation and definition of parameters.

$$\varepsilon = \frac{\sigma}{0.97E} + c \quad (6)$$

From Eqs. (5) and (6), σ_{pl} is derived as:

$$\sigma_{pl} = \left(\frac{3\sigma_{max}^n}{97E\beta} \right)^{1/(n-1)} \quad (7)$$

Since four stress-strain relations were obtained for one test specimen, four values of Young's modulus and proportional limit stress were determined. Three bending strengths were determined since the bending strengths obtained from $\sigma_{eb}-\varepsilon_{dl}$ and $\sigma_{eb}-\varepsilon_g$ coincided with each other.

Numerical analyses considering the material nonlinearity

The influence of deflection was analyzed by a simple numerical technique. Considering the symmetry of the three-point loading test, the analysis can be conducted as a cantilever beam subjected to an end load. The length of the beam, which corresponds to a half span, is uniformly divided into several finite elements. As shown in Fig. 3, the reaction force at the support, N , is supposed to be vertically applied at the end of the cantilever. When the angle between the tangential line and x -axis is defined by θ , the bending equation correspond-

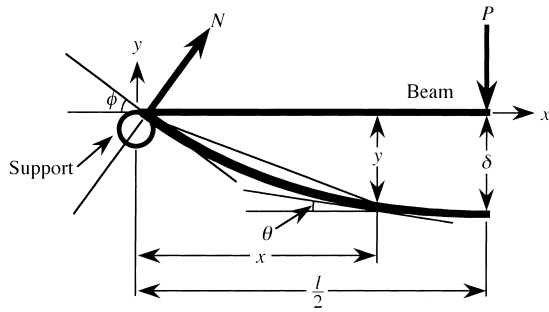


FIG. 3. Bending model used for the numerical analysis.

ing to each element is represented as follows:

$$E'I \frac{\Delta\theta}{\Delta x} = -M = -\frac{P}{2}(x + y \tan \phi) \quad (8)$$

where M is the bending moment, E' is the tangent modulus of the element, I is the secondary moment of inertia of the beam, P is the applied load, and ϕ is the slope angle at the supporting point. The definition of tangent modulus is shown in Fig. 2. From this equation, we can obtain the following relation:

$$\Delta\theta = -\frac{P'}{2E'I}(x + y \tan \phi)\Delta x \quad (9)$$

The angle θ can be determined by summing up $\Delta\theta$ from $x = 0$ to $x = x$. The slope of the deflection curve $\Delta y/\Delta x$ is derived by θ as:

$$\frac{\Delta y}{\Delta x} = \tan \theta \quad (10)$$

From this equation, the vertical displacement y is calculated by summing up $\Delta x \tan \theta$ from $x = 0$ to $x = x$. The angle θ at the end of the beam corresponds to ϕ used in the next stage.

The longitudinal strain ε can be obtained from Eq. (8) as follows:

$$\varepsilon = \frac{Mh}{2E'I} = \frac{Ph(x + y \tan \phi)}{4E'I} \quad (11)$$

The strain increment $\Delta\varepsilon$ is calculated by subtracting the strain at the previous stage from the temporary one, and the stress increment $\Delta\sigma$ is calculated as:

TABLE 2. Parameters determining the nonlinear stress-strain relation.

Species	n	$\beta (\times 10^{-3})$	σ_{\max} (MPa)
Beech	7.2	8.2	100
Western hemlock	9.6	5.1	110

$$\Delta\sigma = E' \Delta\varepsilon \quad (12)$$

The bending stress of each element is calculated using the two different methods. In the one method, the stress was updated by adding $\Delta\sigma$ of Eq. (12) to that in the previous stage. In the other method, the stress was obtained by substituting the applied load P into Eq. (1). Using Ramberg-Osgood's function, which is written as Eq. (5), the tangent modulus E' is converted by the updated stress as follows:

$$E' = \frac{d\sigma}{d\varepsilon} = \left[\frac{1}{E} + \frac{n\beta}{\sigma_{\max}} \left(\frac{\sigma}{\sigma_{\max}} \right)^{n-1} \right]^{-1} \quad (13)$$

From this procedure, the deflection curve and the stress-strain relation corresponding to each element are updated in every stage.

In the calculation, the beam was divided into 20 elements along the long axis. The dimensions of the testing model coincided with those in the real bending tests. In the first stage, the tangent modulus of each element was uniformly given by Young's modulus. Young's modulus and bending strength were derived from the experimental data, whereas the parameters n , β , and σ_{\max} used for Ramberg-Osgood's function were determined from the data of the specimens with the span/depth ratio of 20. Table 2 shows these parameters corresponding to each species. To simplify the calculation, the change of loading direction at the support was considered, and the influence of frictional force and radii of loading and supporting points were ignored. The calculation was repeated until the bending stress at the loading point attained 150 MPa.

RESULTS AND DISCUSSION

Bending tests

In obtaining the strain from the deflection, we used Eq. (4) based on elementary bending

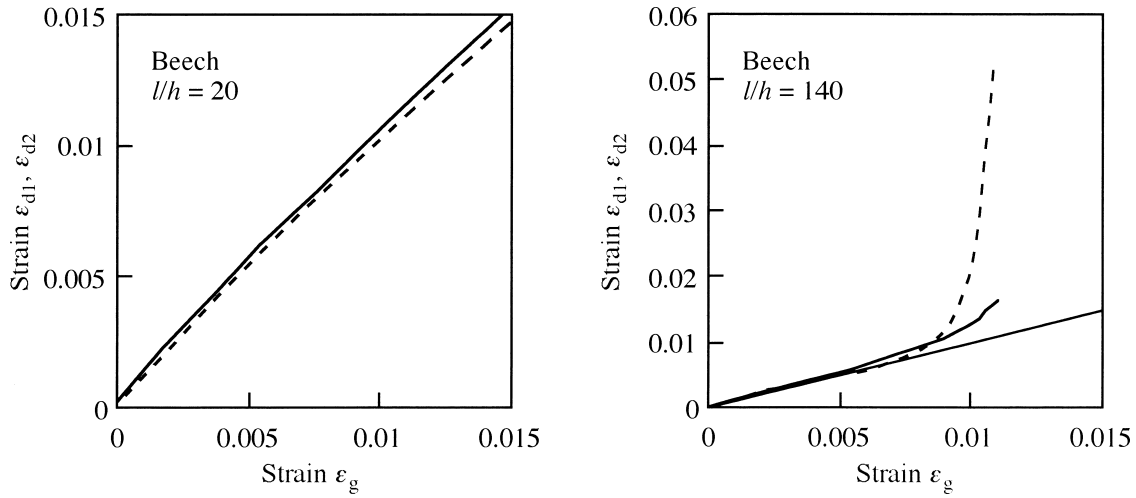


FIG. 4. Comparisons of the strains obtained from different procedures. Strains ε_g , ε_{d1} , and ε_{d2} are obtained from the strain gage output, equation based on elementary bending theory, and equation considering the geometrical non-linearity, respectively. Solid and dashed lines correspond to ε_{d1} and ε_{d2} , respectively.

theory. Nevertheless, the influence of geometrical nonlinearity on the strain can be taken into account as well as that on the bending stress. As for the relation between the deflection and the strain at the midspan, Uemura and colleagues derived the correct equation (Uemura et al. 1978). The corrected strain, which is defined as ε_{d2} , is represented as follows:

$$\varepsilon_{d2} = \frac{6h}{l^2} \delta \left[1 - 12.34 \left(\frac{\delta}{l} \right)^2 + 161.6 \left(\frac{\delta}{l} \right)^4 \right] \times \left[1 + 4 \left(\frac{\delta}{l} \right)^2 \right] \quad (14)$$

Figure 4 shows the strain ε_{d1} and ε_{d2} corresponding to the strain gage output ε_g . When the span/depth ratio was in the lower test range, the values of ε_{d1} and ε_{d2} coincided well with that of ε_g throughout the strain range. When the span/depth ratio was large, however, ε_{d1} and ε_{d2} tended to be larger than ε_g in the large strain range. In particular, the difference between the values of ε_{d2} and ε_g was quite marked when ε_g was larger than 0.01 in spite of the correction. Although ε_{d1} also tended to be larger than ε_g , the difference was smaller than that between ε_{d2} and ε_g . Therefore, for the relation between the deflection and strain at

the midspan, some corrected equation would be more appropriate than Eqs. (4) and (14). In the succeeding discussion, however, we used Eq. (4) for the strain given by the deflection.

Figure 5 shows the typical $\sigma_{eb}-\varepsilon_{d1}$ and $\sigma_{ld}-\varepsilon_{d1}$ relations obtained from the different span/depth ratios. At lower span/depth ratios, these relations were similar to each other. In contrast, the discrepancy between the relations was marked in the large strain region when the span/depth ratio was large. This tendency was applicable to the $\sigma_{eb}-\varepsilon_g$ and $\sigma_{ld}-\varepsilon_g$ relations.

Figure 6 shows the calculated Young's modulus corresponding to the span/depth ratios tested. This figure indicates that the Young's modulus obtained by using the strain gage was larger than that calculated from the vertical displacement using test machine speed and time. When comparing the moduli obtained from the $\sigma_{eb}-\varepsilon_{d1}$ and $\sigma_{ld}-\varepsilon_{d1}$ relations, however, the difference was not significant at any of the span/depth ratios examined here. This tendency was found in the moduli obtained from the $\sigma_{eb}-\varepsilon_g$ and $\sigma_{ld}-\varepsilon_g$ relations.

Figure 7 shows the proportional limit stress corresponding to the test span/depth ratios. The proportional limit stress obtained by using the strain gage output was smaller than that

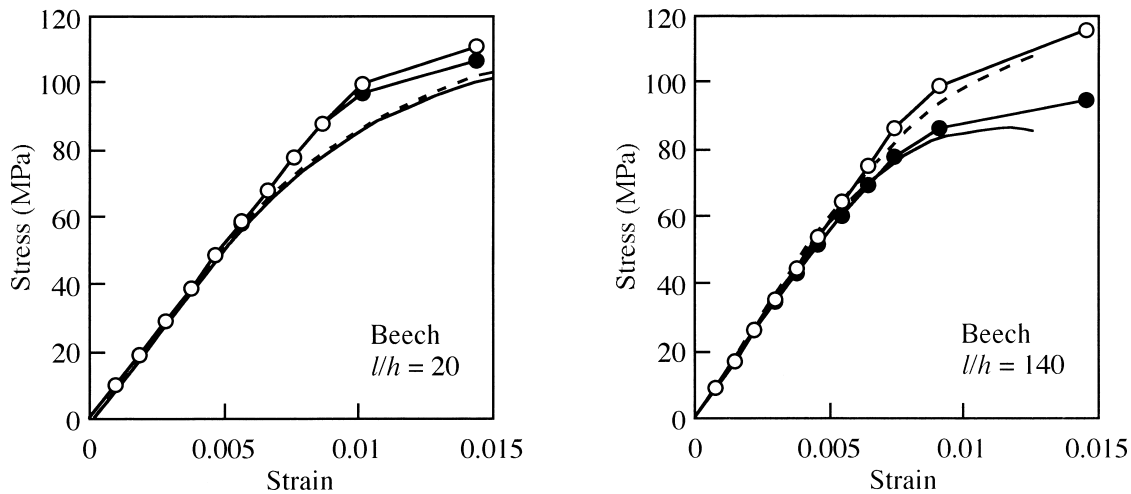


FIG. 5. Typical stress-strain relations obtained by the bending tests and numerical analyses. The solid line and black circles are the experimental and numerical results, respectively, without considering the influence of deflection, whereas the dashed line and white circles are those in which the influence of deflection is taken into account.

measured by vertical displacement when the span/depth ratio range was smaller than 100, whereas this tendency was not significant when the span/depth ratio exceeded 100. We initially thought that the proportional limit stress might be influenced by the deflection because it is determined in the deflection range larger than that used for determining Young's modulus. Nevertheless, the statistical analysis revealed that the influence of deflection was not significant over the entire range of span/depth ratios.

Figure 8 shows the bending strength corresponding to the test span/depth ratios. When the bending stress is derived by elementary bending theory, it is determined independently of the strain measurement. Thus, the influence of the strain measurement on the bending strength exists when the deflection is taken into account. In contrast to the properties mentioned above, the bending strength was not markedly influenced by the measurement of strain at any of the span/depth ratios, whereas it was influenced by the deflection. When the strength was calculated by elementary bending theory, it tended to decrease as the span/depth ratio increased. In contrast, the strength calculated by the equation in which the deflection

is taken into account was stable and independent of the span/depth ratio. Statistical analysis revealed that the decrease of strength obtained by elementary bending theory was marked when the span/depth ratio exceeded 100. Hence, the equation considering the deflection is preferable when the specimen has a span/depth ratio larger than 100. In previous works, it was shown that the span/depth ratio should be larger than 20 for reducing the effect of shearing force (Yoshihara and Matsumoto 1999; Yoshihara et al. in press). Therefore, the span/depth ratio range should be restricted to between 20 and 100 when the bending properties are measured based on elementary bending theory. Otherwise, the equation considering the deflection should be used for measuring the bending strength.

Numerical analyses considering the material nonlinearity

Figure 5 also shows the stress-strain relations at the loading point obtained from the numerical analyses. When the influence of deflection was taken into account, the bending stress was larger than that obtained from elementary bending theory because the additional

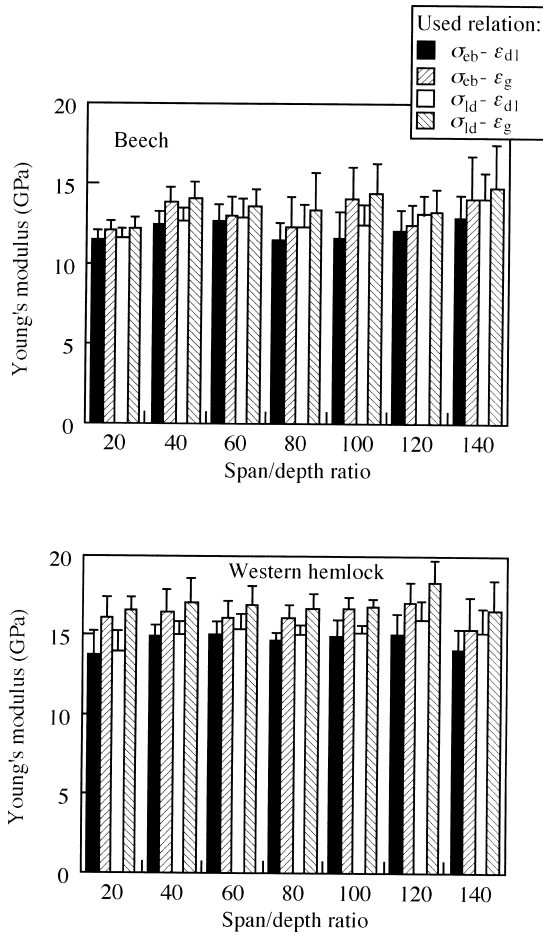


FIG. 6. Young's modulus corresponding to the span/depth ratio. Columns and horizontal bars are the average and standard deviations, respectively.

bending moment caused by the deflection, which is represented by the second term in the parentheses of Eq. (9), was marked with increasing deflection. This additional moment was emphasized when the span/depth ratio was large. The numerical calculations give a rather good approximation of the corresponding stress-strain relations experimentally obtained whether the deflection was taken into account or not. Although several simplifications were introduced, the numerical technique adopted here was effective in predicting the bending behavior.

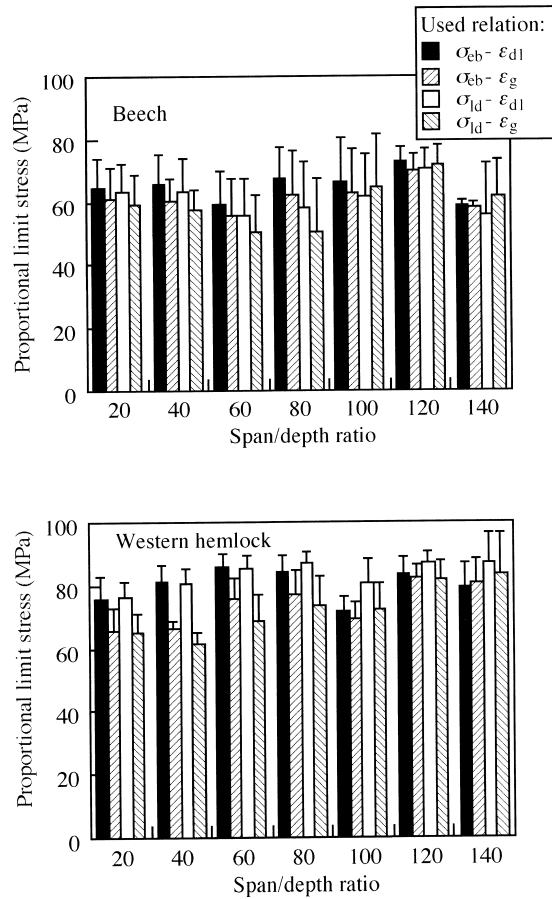


FIG. 7. Proportional limit stress corresponding to the span/depth ratio. See Fig. 6 for further information.

CONCLUSIONS

Using 20- × 5-mm specimens of western hemlock and beech, we examined the influence of large deflection on the measurement of flatwise bending properties, and obtained the following results:

- (1) When the deflection is quite large, the strain at midspan that is calculated from the deflection shows a discrepancy from that measured by the strain gage because the geometrical nonlinearity is significant. Thus it is difficult to estimate the strain at midspan from the deflection.
- (2) Deflection had little influence on the measurement of Young's modulus and propor-

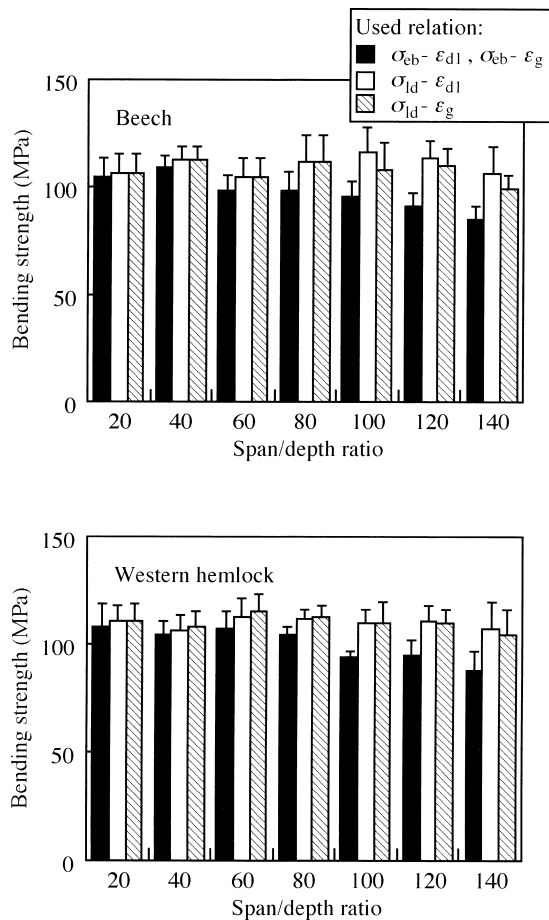


FIG. 8. Bending strength corresponding to the span/depth ratio.

tional limit stress. In contrast, the bending strength obtained by elementary bending theory decreased when the span/depth ratio exceeded 100, whereas that given by the equation considering the deflection was stable throughout the span/depth ratio range examined here.

(3) In using elementary bending theory for

determining the bending properties, the span/depth ratio should be restricted smaller than 100. Otherwise, the equation considering the deflection should be used for measuring the bending strength.

(4) The bending behavior including the influence of large deflection could be well approximated by the simple numerical analysis considering the material nonlinearity.

REFERENCES

- AMERICAN SOCIETY FOR TESTING AND MATERIALS (ASTM). 1997. Standard methods of testing small clear specimens of timber. ASTM D143-94, ASTM. West Conshohocken, PA.
- INTERNATIONAL ORGANIZATION FOR STANDARDIZATION (ISO). 1975. Wood-determination of modulus of elasticity in static bending. ISO 3349-75, ISO. Geneva, Switzerland.
- JAPANESE INDUSTRIAL STANDARD (JIS). 1988. Testing methods for flexural properties of carbon fiber reinforced plastics. K7074-88, JIS. Tokyo, Japan.
- . 1994. Methods of test for woods. JIS Z2101-94, JIS. Tokyo, Japan.
- RAMBERG, W., AND W. R. OSGOOD. 1943. Description of stress-strain curves by three parameters. NACA TN-902.
- SAWADA, M. 1955. Studies on the mechanics of wood beams III. Load-deflection curves in wood beams of rectangular cross section. Bull. Jpn. Gov. For. Exp. Sta. 77:69–102.
- UEMURA, M. 1981. Problems in characterizing the mechanical properties of fiber reinforced plastics and the standard for designing (II). J. Jpn. Soc. Composite Mater. 7:74–81.
- , K. IYAMA, AND Y. YAMAGUCHI. 1978. Examination of the bending test method of fiber reinforced plastics. Kyoka Plastics 24:13–20.
- YOSHIHARA, H., AND S. MATSUMOTO. 1999. Examination of the proper span/depth ratio range in measuring the bending Young's modulus of wood based on the elementary beam theory. Mokuzai Kogyo 54:269–272.
- , Y. KUBOJIMA, AND T. ISHIMOTO. 2003. Several examinations on the static bending test methods of wood by using todomatsu (Japanese fir). Forest Prod. J. (in press.)